Thermodynamic Characterization of the DmsD Binding Site for the DmsA Twin-Arginine Motif

ARTICLE *in* BIOCHEMISTRY · FEBRUARY 2015

Impact Factor: 3.02 · DOI: 10.1021/bi500891d · Source: PubMed

2 AUTHORS:

Tara Winstone
The University of Calgary
19 PUBLICATIONS **277** CITATIONS
SEE PROFILE

Raymond J. Turner
The University of Calgary
172 PUBLICATIONS **4,525** CITATIONS
SEE PROFILE

BIOCHEMISTRY
including biophysical chemistry & molecular biology

Article

pubs.acs.org/biochemistry

Thermodynamic Characterization of the DmsD Binding Site for the DmsA Twin-Arginine Motif

Tara M. L. Winstone and Raymond J. Turner*

Department of Biological Sciences, University of Calgary, 2500 University Drive Northwest, Calgary, AB, Canada T2N 1N4

Supporting Information

ABSTRACT: The system specific chaperone DmsD interacts with the twin-arginine leader peptide of its substrate, DmsA, allowing for proper folding and assembly of the DmsA catalytic subunit of dimethyl sulfoxide reductase prior to translocation by the twin-arginine translocase. DmsD residues important for binding the complete 45-amino acid sequence of the DmsA leader (DmsAL) peptide were previously identified and found to cluster in a pocket of the DmsD structure. In this study, we have utilized isothermal titration calorimetry (ITC) to determine the dissociation constant and thermodynamic parameters of 15 single-substitution DmsD variant proteins and a synthetic DmsAL peptide consisting of 27 amino acids ($DmsAL_{15-41}$). The stoichiometry values were determined via ITC, and the multimeric compositions of the DmsD variants in the absence and presence of peptide were characterized via size exclusion chromatography and native polyacrylamide gel electrophoresis. An up to 4-fold change in affinity was observed for DmsD variant proteins relative to that of wild-type DmsD, and variation of the entropic contribution to binding divided the binding site into two clusters: residues with either more or less favorable entropy. Substitution of hydrophobic residues along one helix face (helix 5) or prolines found on adjacent loops caused reduced binding affinity because of the increased entropic cost, which suggests that the twin-arginine motif of the DmsAL peptide binds to a preformed site on DmsD. Most DmsD variants were more than 90% monomeric in solution and bound a single peptide per protein molecule. The DmsD variant with the largest dimer population showed increased affinity and induced the formation of tetramers in the presence of peptide, suggesting that dimeric DmsD or an alternatively folded form of DmsD may play an as yet undefined role in binding.

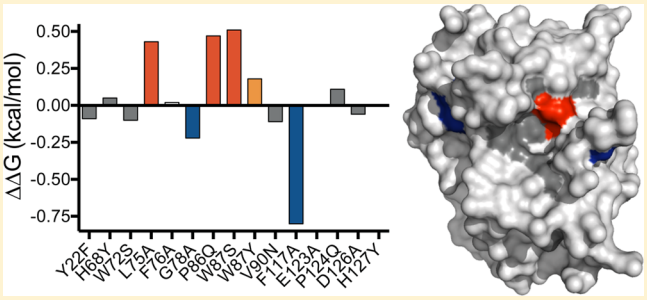

Coordinating the events involved in folding, assembly, and targeting of enzyme complexes is important to all biological systems. In bacteria, the generation of energy by a variety of respiratory electron transport chains is essential, given the diverse environments in which they are often found. The *Escherichia coli* twin-arginine translocase (Tat) facilitates transport of folded proteins across the inner membrane through recognition of a twin-arginine (RR) sequence motif within the N-terminal leader peptide of a Tat substrate protein.[1−5] Many Tat substrates are components of multi-subunit redox respiratory enzymes that acquire complex cofactors such as molybdopterin (MoPt) and iron−sulfur (Fe−S) clusters, in addition to folding and often assembling with a partner protein prior to translocation by the Tat complex.[6] System specific chaperones, also termed redox enzyme maturation proteins (REMPs), play an important role in the maturation process of their cognate Tat substrate.[7] Each REMP binds specifically to its Tat substrate with very little cross-recognition;[8] however, some REMPs do contain binding sites for both the mature protein substrate and the N-terminal twin-arginine leader peptide.[9] Some unifying themes have become apparent in the interactions between REMPs and their Tat substrate; however, the nature of the binding and REMP mechanism may be unique to each enzyme system.

The DmsD/TorD family of molybdoprotein REMPs has been the most extensively studied to date and includes DmsD, TorD, and NarJ.[10] DmsD allows for maturation of the dimethyl sulfoxide (DMSO) reductase enzyme (DmsABC)[11,12] through binding to the twin-arginine leader peptide of DmsA.[9] TorD assists in the maturation of trimethylamine *N*-oxide (TMAO) reductase (TorAC)[13−18] and contains a binding site for both the TorA leader peptide and the TorA mature protein.[9,19] The maturation of nitrate reductase A (NarGHI) is dependent upon NarJ.[20−22] The N-terminal region of NarG contains a vestige Tat leader peptide[23] that is recognized by NarJ. The REMP of each Tat substrate is believed to play a role in the folding, cofactor loading, assembly, and targeting to the Tat translocase, allowing functionality of each reductase enzyme complex.

It is now established that the hydrophobic region of the Tat substrate leader peptide is the most important determinant of binding specificity for both DmsD and TorD.[24−26] A synthetic peptide composed of residues 15−41 of the 45-amino acid DmsA leader (DmsAL) peptide was shown to bind to DmsD with micromolar affinity (1.7 μM), and the minimal binding

Received: January 24, 2014
Revised: February 5, 2015

DOI: 10.1021/bi500891d
Biochemistry XXXX, XXX, XXX−XXX

unit of the DmsAL peptide was shown to be the hydrophobic region ($DmsAL_{21-41}$).[24] A putative RR leader peptide binding site was identified using an immunoblot far-Western technique to assess binding of DmsD single-substitution variant proteins and a modeled structure of DmsD.[27] Subsequently, the structure of the *E. coli* DmsD (EcDmsD) protein was reported, and amino acids previously shown to be important for binding were found clustered within a hydrophobic pocket of the structure.[28]

Three-dimensional structures of all three molybdo-enzyme REMPs have been determined and illustrate that this family of proteins have a very similar architecture despite the subtle differences in binding behavior toward their Tat substrate. *Shewanella massilia* TorD [Protein Data Bank (PDB) entry 1N1C] was the first REMP structure published and contains a unique fold in which the protein has N- and C-terminal globular helical domains attached via a hinge region composed of conserved residues. The two globular helical domains undergo domain swapping such that the N-domain (residues 1−129) from one polypeptide interacts with the C-domain (residues 130−211) of another TorD polypeptide with each globular domain composed of 10 α-helices.[29] The structure of the *Archaeoglobus fulgidus* NarJ protein homologue was also determined (PDB entry 2O9X) but as a monomer containing 10 α-helices.[30] Four protein structures are available for DmsD, one from *Salmonella typhimurium* (PDB entry 1S9U)[31] and three from *E. coli* (PDB entries 3EFP, 3CWO, and 3U41).[28,32] In all four DmsD structures, the protein shows an all α-helical structure (11 α-helices) with an organization similar to that of a monomeric unit of the SmTorD and AfNarJ homologues. Amino acid residues conserved across this family of proteins cluster within a pocket comprised of the intersection of three loops (one of which corresponds to the aforementioned hinge region of the SmTorD domain-swapped dimer) and the face of one helix.[28] Multiple studies have shown this pocket of conserved residues to be important for binding to the twin-arginine leader peptide substrate;[10,26−28,32−34] however, the effect of each of the residues on the strength and nature of the binding has not been thoroughly characterized.

DmsD and TorD proteins have been shown to form dimers and higher-order oligomers as well as exist in a "low-pH" folded form.[35,36] Both DmsD and TorD low-pH forms were shown to have secondary structural content similar to that of the native monomer and dimer but were resolved as multiple bands on a native PAGE gel.[35,36] Research has also confirmed that both SmTorD and EcDmsD are capable of binding their RR leader peptide substrate as either a monomer or a dimer,[35,36] but the stoichiometry of binding was not determined. Despite the structural and binding information that is available, a complex of a DmsD/TorD protein member with its Tat substrate has not been determined.

To improve our understanding of the nature of the interaction between the DmsD REMP and its substrate, the DmsA RR leader peptide; isothermal titration calorimetry (ITC) was used to characterize 14 residues within the DmsD putative binding pocket. Affinity and thermodynamic parameters were determined between 15 single-substitution DmsD variant proteins and a synthetic peptide composed of a portion of the DmsA leader peptide ($DmsAL_{15-41}$). The hydrodynamic behavior of the DmsD variant proteins was characterized via size exclusion chromatography (SEC) and native PAGE (nPAGE) and compared with stoichiometry results from ITC to determine if the different forms of DmsD might influence binding behavior. Up to 4-fold changes in affinity were observed for the DmsD variants relative to that of the wild-type protein; however, the variation in the entropic contribution to binding divided the binding site into two distinct clusters, those residues with more favorable and those with less favorable entropy changes. The results illustrate the importance of neutral residues in DmsD to the binding of the DmsAL peptide and also show support for an interaction between a conserved glutamate residue (E123) and the first arginine (R16) of the leader peptide. Wild-type DmsD and most of the DmsD variants were more than 90% monomeric; however, the DmsD variant with larger amounts of dimer also showed increased binding affinity and the formation of tetramers upon binding the peptide, suggesting a role for alternatively folded or dimeric DmsD protein.

MATERIALS AND METHODS

Site-Directed Mutagenesis. Fourteen single-site mutations were made to 13 residues in *dmsD*. The rationale behind the selection of these 13 residues is outlined in Table 1 and was detailed previously.[27] The choice of amino acid substitution at a given residue position was made on the basis of a guide for "safe" substitutions in site-directed mutagenesis[37] as a structure was not available at the time of selection. Single-residue mutations were generated using the QuikChange II Site-Directed Mutagenesis kit (Stratagene) with 25 ng of pTDMS67[38] as a template following the manufacturer's instructions. The resulting recombinant plasmids were isolated using a Plasmid Midi kit (Qiagen) and verified by sequencing (University Core DNA Services, University of Calgary) prior to transformation into *E. coli* C41(DE3) by heat shock.[39]

Table 1. DmsD Variant Proteins Selected for Characterization of Binding with the DmsA Leader Peptide ($DmsAL_{15-41}$)

variant	selection[b]	location[c]	simulation[d]	$\Delta\delta$ (with $DmsAL_{1-44}$)[e]
Y22F[a]	D	α1	V(L19)	<0.2 ppm
H68Y[a]	T	α5	H(T22)	<0.1 ppm
W72S[a]	R	α5	V(V20)	<0.1 ppm
L75A[a]	D R	α5		undefined
F76A[a]	D R	α5	H V(G18, L19)	undefined
G78A	D	L5		undefined
P86Q[a]	D	L5		undefined
W87Y[a]	D	L5		undefined
W87S	D	L5		undefined
V90N	D	α6		<0.1 ppm
F117A		L7		>1.0 ppm
E123A[a]	D R	L7	H V(R16)	unknown parts per million
P124Q[a]	D	L7		undefined
D126A[a]	D R T	L7		<0.1 ppm
H127Y[a]	R T	L7	V(L19)	<0.1 ppm

[a]Residues in DmsD selected on the basis of sequence homology[10] and binding previously studied using an immunoblot assay.[27] [b]Selection of residue for mutation was based on sequence homology with (D) DmsD proteins, (R) REMP family proteins, or (T) THEMATICs. [c]Location of residue within the EcDmsD structure (PDB entry 3EFP): α, α-helix; L, loop. [d]Proposed interactions from a docking and simulation experiment with the DmsA leader peptide: H, H-bond; V, van der Waals (DmsAL residue).[28] [e]Chemical shift of the DmsD residue in the presence of $DmsAL_{1-44}$ at pH 6.5.[44]

DOI: 10.1021/bi500891d
Biochemistry XXXX, XXX, XXX−XXX

DmsD Protein Expression and Purification. Recombinant wild-type (WT) and single-substitution variant DmsD proteins were expressed and purified as explained previously.[38] Overnight cultures were diluted 1% into LB broth containing ampicillin (100 μg/mL), grown at 37 °C to mid log phase (A_{600} = 0.5), and induced with a final IPTG concentration of 0.5 mM for 3 h at room temperature (~25 °C). Cells were harvested by centrifugation, washed with lysis buffer [50 mM Tris-HCl (pH 7.5), 1 M NaCl, 5 mM imidazole, and 2 mM DTT], collected, resuspended in lysis buffer (1 mL/g), and stored as a frozen cell slurry at −80 °C. The cell slurry was thawed, and additional lysis buffer was added (1 mL/g) prior to cell breakage with two passes through a French press cell at 16000−18000 psi. Unbroken cells were removed from the lysate by centrifugation at 10000*g* for 30 min.

DmsD proteins were purified from the cell free lysate with nickel affinity chromatography using a GE Biosciences 5 mL HisTrapFF column on an AKTA Purifier system. Lysate was applied to the column in 10 mL batches of 20 mg/mL lysate in lysis buffer. Five column volumes of wash buffer containing 35 mM imidazole were used to remove contaminant proteins. Monomeric DmsD protein eluted with a 125 mM imidazole step gradient, while dimeric DmsD protein required 250 mM imidazole to elute. WT and variant DmsD proteins routinely contained small amounts of dimeric protein, while some variant proteins were seen to contain more or less protein eluting as a dimer. For all calorimetric and subsequent studies, only the monomeric (low imidazole eluted) DmsD protein was used for analysis to keep the preparations consistent. DmsD proteins eluted from the nickel affinity column were pooled and exchanged into storage buffer [25 mM Tris-HCl (pH 8.0), 100 mM NaCl, and 1 mM DTT] by application onto a 5 mL HiTrap column and collection of eluted fractions. Samples were concentrated with Amicon 10 kDa cutoff filters, and the purity was determined via SDS−PAGE prior to being stored at −20 °C.

Isothermal Titration Calorimetry. In preparation for ITC experiments, purified DmsD protein samples were thawed in a room-temperature water bath for 5 min, vortexed, and centrifuged at 10000*g* for 10 min at 4 °C to remove insolubles. The protein concentration was determined by absorbance at 280 nm using a theoretically determined extinction coefficient (online ExPASy tool ProtParam available at http://web.expasy.org/protparam/)[40] as well as a Bradford assay. Comparison of protein concentrations determined prior to storage with those determined following thawing showed that recovery was routinely greater than 90% for all DmsD proteins. The soluble protein was exchanged into ITC buffer [25 mM Tris-HCl (pH 8.0) and 100 mM NaCl] by application onto two 5 mL HiTrap columns (GE Biosciences) connected in series and collection of eluted fractions. The protein concentration was determined from absorption at 280 nm. DmsD proteins were diluted to ~25 μM with ITC buffer and prepared in 10 mL batches to allow for triplicate titrations. For each titration, 3 mL of a 25 μM DmsD solution was degassed with a thermovac at 28 °C for 10 min. The ITC sample cell was loaded with a degassed DmsD sample, and the sample remaining in the syringe after filling was used to confirm the protein concentration with a Bradford assay and the absorbance at 280 nm.

DmsA leader (DmsAL) peptide containing amino acid residues 15−41 ($DmsAL_{15-41}$) was chemically synthesized and purified to 95% purity by GenScript. This peptide was shown previously to bind to WT DmsD.[24] ^{1}H NMR spectroscopy of the DmsAL peptide, compared to an internal standard [4,4-dimethyl-4-silapentane-1-sulfonic acid (DSS)], was used to determine that 70% of the lyophilized peptide mass corresponded to peptide mass.[24] $DmsAL_{15-41}$ peptide was weighed on an analytical balance and dissolved in distilled water to a concentration of 0.5 mM, diluted to 0.25 mM with 2× ITC buffer, and stored at 4 °C prior to titration. For each titration experiment, a 0.5 mL peptide sample was degassed and equilibrated to 28 °C for 10 min with a thermovac and then loaded into the ITC syringe.

ITC experiments were performed on a MicroCal VP-ITC microcalorimeter at 30 °C (303.15 K). Twenty-nine 10 μL injections of 250 μM DmsAL peptide were added to 25 μM DmsD protein. Titrations were performed in triplicate for each DmsD variant protein, and the heat of dilution (peptide ligand into buffer) was subtracted from the individual heats of reaction to obtain the observed heat of binding. Origin 7.0 was used for data fitting with a single-binding site model. The mean and standard error of dissociation constants and corresponding thermodynamic parameters were determined and reported (Table 2).

Table 2. Thermodynamic Parameters for $DmsAL_{15-41}$ Peptide Binding to DmsD Variant Proteins

DmsD[a]	K_d (μM)[b]	ΔG (kcal/mol)[b]	ΔH (kcal/mol)[b]	$-T\Delta S$ (kcal/mol)[b]
W87S	3.7 ± 0.5	−7.5 ± 0.2	−12.4 ± 1.1	4.9 ± 1.2
P86Q	3.6 ± 0.2	−7.5 ± 0.1	−12.4 ± 0.2	4.9 ± 0.2
L75A	3.4 ± 0.7	−7.6 ± 0.1	−13.0 ± 0.6	5.4 ± 0.7
W87Y	2.3 ± 0.4	−7.8 ± 0.1	−9.1 ± 0.6	1.3 ± 0.7
P124Q	2.0 ± 0.1	−7.9 ± 0.1	−12.9 ± 1.4	5.0 ± 1.4
H68Y	1.8 ± 0.2	−8.0 ± 0.1	−12.5 ± 0.2	4.5 ± 0.2
F76A	1.8 ± 0.3	−8.0 ± 0.1	−12.8 ± 0.4	4.8 ± 0.5
WT	1.7 ± 0.2[c]	−8.0 ± 0.1[c]	−11.7 ± 0.2[c]	3.7 ± 0.2[c]
E123A	1.7 ± 0.8	−8.0 ± 0.2	−6.2 ± 0.8	−1.8 ± 0.6
H127Y	1.6 ± 0.2	−8.0 ± 0.1	−10.7 ± 0.1	2.7 ± 0.2
D126A	1.6 ± 1.2	−8.0 ± 0.3	−11.7 ± 0.9	3.7 ± 1.2
Y22F	1.5 ± 0.2	−8.1 ± 0.1	−10.3 ± 0.2	2.3 ± 0.2
W72S	1.5 ± 0.7	−8.1 ± 0.2	−11.8 ± 0.8	3.7 ± 0.9
V90N	1.4 ± 0.2	−8.1 ± 0.2	−10.4 ± 0.2	2.3 ± 0.2
G78A	1.2 ± 0.1	−8.2 ± 0.1	−10.9 ± 0.8	2.7 ± 0.8
F117A	0.4 ± 0.1	−8.8 ± 0.1	−11.4 ± 0.2	2.6 ± 0.2

[a]DmsD variant proteins are listed from weakest to tightest binding (largest to smallest K_d). [b]ITC experiments were performed in triplicate at 30 °C in Tris-HCl (pH 8.0). Mean and SEM values are reported for the dissociation constant (K_d) and free energy (ΔG), enthalpy (ΔH), and entropy ($-T\Delta S$) of binding. [c]Previously reported.[24]

Size Exclusion Chromatography. SEC was used to investigate the multimeric states of the DmsD proteins in solution. DmsD WT and variant proteins prepared for ITC were also subjected to SEC on an AKTA Purifier system. Where possible, samples with peptide added (collected after ITC experiment) were also analyzed by SEC. Prior to SEC, samples were centrifuged at 10000 rpm for 10 min at 4 °C to remove any trace precipitation. A 100 μL sample was loaded onto a Superose 12 column (GE Biosciences) equilibrated with ITC buffer [25 mM Tris-HCl (pH 8.0) and 100 mM NaCl]; samples were run at 0.5 mL/min, and elution was monitored at 220 nm. The column was calibrated with globular proteins with known molecular masses [albumin (67 kDa), ovalbumin (43

DOI: 10.1021/bi500891d
Biochemistry XXXX, XXX, XXX−XXX

kDa), α-chymotrypsinogen (25 kDa), and ribonuclease A (13.7 kDa)]. Blue dextran was used as a marker of void volume, and methyl-trytophan ester was used to determine the total volume of the column. Monomeric DmsD eluted with 13.6 mL, and dimeric DmsD (when present) eluted with 12.2 mL. The elution volumes and determined apparent molecular masses (26.9 and 51.8 kDa) agreed with the formula weights of the recombinant DmsD constructs (27.5 and 55 kDa, respectively). Sample chromatograms are shown in Figure 5.

SDS and Native Polyacrylamide Gel Electrophoresis. Protein samples were resolved on a Bio-Rad Mini Protein II or ATTO apparatus using a 4% acrylamide stacking gel and a 12% acrylamide separating gel as described previously.[41,42] Protein samples were resuspended in SDS−PAGE loading buffer [50 mM Tris-HCl (pH 6.8), 2% (w/v) SDS, 100 mM DTT, 40% (w/v) glycerol, and 0.2% bromophenol blue] and heated at 100 °C for 5 min prior to being loaded onto an SDS−PAGE gel. Bio-Rad low-molecular weight protein standards were used to determine the approximate molecular weight of resolved protein bands. Gels were fixed, stained with Coomassie Blue, and destained prior to image capture. DmsD protein samples were also resolved on an ATTO apparatus with an nPAGE gel (4% stacking, 12% separating). Preparation for nPAGE was done as described above with the exclusion of SDS from all buffers. Samples were resuspended in nPAGE loading buffer [50 mM Tris-HCl (pH 6.8), 40% glycerol, and 0.2% bromophenol blue] at room temperature for 15 min prior to loading. In the indicated cases, dithiothreitol (DTT) was either present or absent from the loading buffer.

Molecular Structure Representation. Figures containing molecular structures were prepared with Pymol Molecular Graphics system version 1.0[43] and used the EcDmsD structure (PDB entry 3EFP).[28]

RESULTS

Selection of DmsD Residues for Characterization of Binding to DmsA Twin-Arginine Leader Peptide. Following sequence analysis of a variety of REMP proteins, conserved motifs and regions of homology within DmsD/TorD proteins were identified.[10] Twenty conserved residues in DmsD were selected for site-directed mutagenesis, and because it was prior to a DmsD protein structure being available, amino acid substitutions were chosen so that the structure was not disrupted.[37] The 20 resulting single-substitution DmsD variant proteins were expressed, purified, and characterized for binding to the complete DmsA leader peptide (residues 1−42) with an immunoblot assay.[27] Eleven of the 20 selected residues clustered together in a pocket on or near the surface of an EcDmsD modeled structure, and most were shown to impact binding of the complete DmsA leader peptide. The EcDmsD structure (PDB entry 3EFP) was later determined and confirmed the localization of these 11 residues to a pocket on or near the surface of DmsD.[28] Docking and simulation experiments conducted with DmsD and the DmsAL peptide substrate supported residues located in the pocket of DmsD interacting with residues of the DmsAL peptide through hydrogen bonding or van der Waals interactions (Table 1).[28] For the study presented here, four additional single-substitution DmsD variants were made on the basis of the proximity to the putative twin-arginine leader peptide binding site pocket and added to the 11 DmsD variants identified and characterized in our previous work.[27] The location of the 14 amino acid residues within the EcDmsD protein structure and sequence are illustrated in panels A and B of Figure 1, respectively, and listed in Table 1. In a recently conducted study, NMR was used to investigate the structural changes in DmsD upon binding to the DmsAL peptide.[44] Chemical shift changes observed for the DmsD residues within the DmsD−DmsAL complex have been included in Table 1 for comparison. Various regions of the complete (45-amino acid) DmsA leader peptide were assayed for binding to WT DmsD with ITC, and a 27-amino acid region ($DmsAL_{15-41}$) was identified to bind with micromolar affinity.[24] To understand the nature of binding between each of the residues within the putative twin-arginine leader peptide binding site, each of the 15 DmsD variant proteins was characterized via ITC with this same portion of the DmsA leader peptide sequence ($DmsAL_{15-41}$) (Figure 1C).

Thermodynamics of Interaction between DmsD Variant Proteins and $DmsAL_{15-41}$ Peptide. A synthetic peptide derived from the DmsA RR leader sequence ($DmsAL_{15-41}$) was shown to bind WT DmsD with a dissociation constant (K_d) of 1.7 μM.[24] The same DmsA leader peptide sequence (Figure 1C) was used here to evaluate the binding of each of the 14 single-substitution DmsD variant proteins (Table 1) by ITC. The thermodynamic data determined from ITC experiments of WT DmsD and variant proteins are listed from weakest to tightest binding (largest to smallest K_d) in Table 2. The weakest binding W87S, P86Q, and L75A DmsD variants had K_d values above 3.4 μM, showing binding more than 2-fold weaker than that of WT DmsD. Other DmsD residues found to have reduced binding affinity included W87Y and P124Q with K_d values of 2.3 and 2.0 μM, respectively. These variants bound to the DmsAL peptide with affinity 1.2-fold weaker than that of WT DmsD. Five DmsD variants bound with affinity very similar to that of WT: H68Y, F76A, E123A, H127Y, and D126A. These DmsD variants had K_d values ranging from 1.8 to 1.6 μM and bound ≤1.2-fold weaker or tighter than WT DmsD. Three DmsD variants (Y22F, W72S, and V90N) showed slightly enhanced binding affinity. The tightest binding DmsD variants, G78A and F117A, had K_d values of 1.2 and 0.4 μM, respectively, corresponding to binding 1.4- and 4.2-fold tighter, respectively, than that of WT (Table 2).

Wild-type DmsD binds to $DmsAL_{15-41}$ peptide with a free energy of −8.0 kcal/mol[24] (Table 2). The weakest binding variant proteins W87S, P86Q, and L75A bound with a free energy of around −7.5 kcal/mol, a decrease of 0.5 kcal/mol from that of WT binding. The tightest binding F117A DmsD variant protein bound with a free energy of −8.8 kcal/mol, an increase of 0.8 kcal/mol favorable free energy. WT DmsD binds to $DmsAL_{15-41}$ with an enthalpy of −11.7 kcal/mol, while the entropy of binding (considered as "$-T\Delta S$") is +3.7 kcal/mol. The binding of $DmsAL_{15-41}$ to DmsD at pH 8.0 is therefore driven by favorable enthalpy accompanied by an entropic cost. When the thermodynamic parameters of each of the DmsD variants were compared and aligned from least to most favorable free energy with corresponding enthalpy and entropy values, an overall trend was not immediately apparent (Table 2). With a closer look, it was noticed that six of the eight DmsD variants with more favorable free energy also had a smaller entropic cost of binding compared to that of WT. The exceptions to this trend included W72S and D126A DmsD, which both had an entropic cost equivalent to that of WT. Six of the seven DmsD variants that bound with a free energy less favorable than that of WT had a larger entropic cost of binding; the only exception was W87Y DmsD.

DOI: 10.1021/bi500891d
Biochemistry XXXX, XXX, XXX−XXX

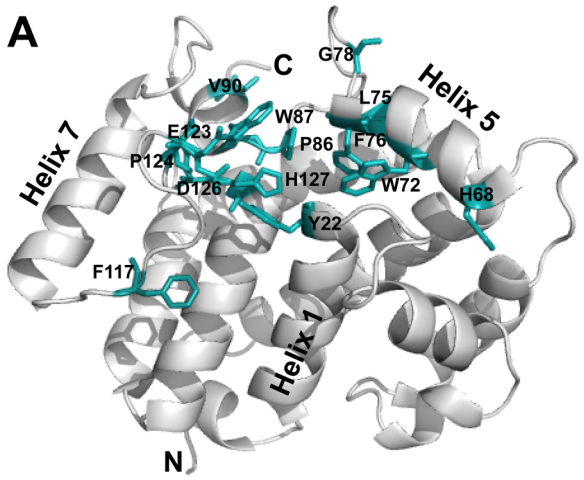

B

```
  1        10         20         30
  MTHFSQQDNFSVAARVLGALFYYAPESAEA
                Helix 1
 31        40         50         60
  APLVAVLTSDGWETQWPLPEASLAPLVTAF

 61        70         80         90
  QTQCEETHAQAWQRLFVGPWALPSPPWGSV
                Helix 5
 91       100        110        120
  WLDRESVLFGDSTLALRQWMREKGIQFEMK
                Helix 7
121       130        140        150
  QNEPEDHFGSLLLMAAWLAENGRQTECEEL

151       160        170        180
  LAWHLFPWSTRFLDVFIEKAEHPFYRALGE

181       190        200
  LARLTLAQWQSQLLIPVAVKPLFR
```

C

```
 15        25         35
  SRRGLVKTTAIGGLAMASSALTLPFSR
        DmsAL15-41
```

Figure 1. Location in the structure and sequence of amino acid substitutions of DmsD protein and DmsA leader peptide sequence. (A) *E. coli* DmsD tertiary structure (PDB entry 3EFP) cartoon diagram with 13 amino acid residues selected for substitution colored teal represented as sticks. (B) Primary sequence of DmsD with 13 amino acid substitutions indicated in bold. Amino acids located within α-helical structure are underlined. Three structural regions of the protein contained multiple substitutions, α-helix 5 (His68, Trp72, Leu75, and Phe76), loop 5 (Gly78, Pro86, and Trp87), and loop 7 (Phe117, Glu123, Pro124, Asp126, and His127). (C) Amino acid sequence of $DmsAL_{15-41}$ peptide.

The almost equivalent free energy but comparatively large differences in entropy of binding are more easily visualized when the variant proteins are reordered from the lowest to highest entropy of binding (Figure 2). With the exception of

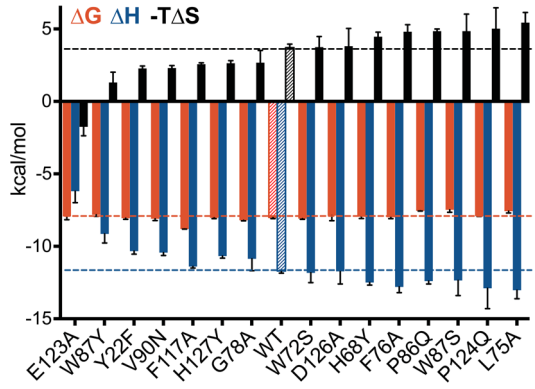

Figure 2. Thermodynamic contributions of binding between single-substitution DmsD variant proteins and $DmsAL_{15-41}$ peptide. The Gibbs free energy (ΔG), entropy ($-T\Delta S$), and enthalpy (ΔH) of binding were determined via isothermal titration calorimetry at 30 °C in 25 mM Tris-HCl (pH 8.0) and 100 mM NaCl. The mean and standard error of triplicate experiments are shown. Variant proteins are shown in order of increasing entropic cost with respective enthalpy and free energy. ΔG, ΔH, and $-T\Delta S$ values for WT DmsD are indicated as dashed lines across the bar graph. Numerical values are listed in Table 3.

one variant (W87Y), the change in free energy of binding also correlated with a change in the entropic cost of binding relative to WT DmsD. This is shown in the DmsD variant proteins that have an increased affinity, in that the binding is less exothermic but more favorable because of the more favorable entropy (i.e., reduced level of order) of binding. The one exception, W87Y, is affected by a larger shift in enthalpy, and while E123A DmsD binds to $DmsAL_{15-41}$ with a free energy equivalent to that of WT (−8.0 kcal/mol), there is a substantial shift in the contributions from entropy and enthalpy, a large loss of favorable enthalpy (+5.5 kcal/mol) with an equivalent gain in favorable entropy relative to WT DmsD (Figure 2 and Table 2). This behavior can be contrasted with that of D126A DmsD, which had the same free energy of binding as WT and also showed the same enthalpic and entropic contributions.

Comparison of the Enthalpy and Entropy of Binding for Each DmsD Variant. The results obtained for the thermodynamics of DmsA RR leader peptide binding showed some apparent exchange of enthalpy to entropy in binding for some DmsD variants (Table 2 and Figure 2). Further analysis of the thermodynamic results was undertaken to explore additional trends in DmsD variant binding. The change in enthalpy ($\Delta\Delta H$) was plotted against the change in entropy ($-T\Delta\Delta S$) for each DmsD variant relative to WT (Figure 3). There is a direct correlation such that the most favorable entropy correlated to the most unfavorable enthalpy, with the slope of the line slightly lower than −1 (−0.94; R^2 = 0.97). In general, if the DmsD variant had a higher entropic cost, the favorable enthalpy was unable to compensate and the overall free energy was reduced, leading to weaker binding. This can be seen in Figure 3 for the DmsD variants with the weakest dissociation constants (W87S, P86Q, and L75A). Alternatively, if the DmsD variant had a reduced entropic cost of binding, this generally meant equivalent or tighter binding as the lost favorable enthalpy was outweighed. Only one exception did not match this generalization; W87Y had a reduced entropic cost,

DOI: 10.1021/bi500891d
Biochemistry XXXX, XXX, XXX−XXX

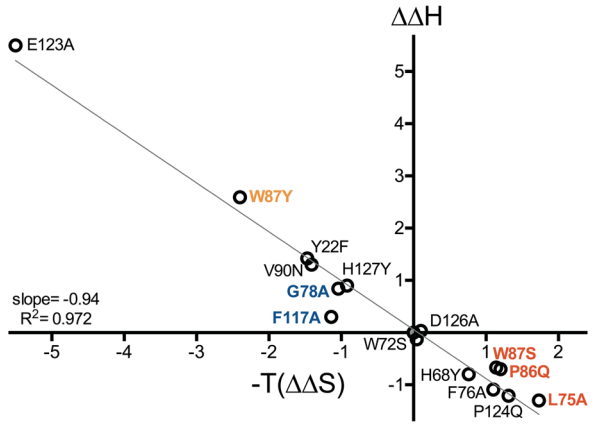

Figure 3. DmsD variant $-T\Delta\Delta S$ vs $\Delta\Delta H$ relative to WT DmsD. Empty circles (Y22F, W72S, G78A, V90N, F117A, E123A, D126A, and H127Y) indicate those variants with ΔG values more favorable than that of WT, and filled circles (W87Y, W87S, H68Y, P86Q, F76A, P124Q, and L75A) indicate those variants with ΔG values less favorable than that of WT. Variants with the most favorable ΔG (F117A and G78A) are colored blue (0.8 and 0.2 kcal/mol more favorable than that of WT). Variants with ΔG values similar to that of WT (within 0.1 kcal/mol) are colored black. Four variants with the most reduced ΔG values are colored orange (0.2 kcal/mol less favorable) or red (0.4−0.5 kcal/mol less favorable).

but the slightly larger reduction of favorable enthalpy caused a reduced free energy and therefore weaker binding (Figure 3).

To observe possible trends in binding behavior on the molecular structure, residues were colored according to their entropy of binding relative to that of WT (Figure 4). DmsD variants with an increased entropic cost of binding, relative to that of WT, were found to cluster on one face of helix 5 and at the intersection of two loops (between helices 5 and 6 and helices 7 and 8) (Figure 4A). The residues that encouraged more disorder (favorable entropy) were predominantly found to cluster at the ends of helices 1 and 6 and the loop between helices 7 and 8, arranged antiparallel within the structure (Figure 4B).

Stoichiometry of Binding and Hydrodynamic Characterization of DmsD Variant Proteins. DmsD has been shown previously to exist as a population of both monomeric and dimeric protein as well as other folded forms.[36] When WT DmsD and variant proteins were prepared for this study, the purification methodology was optimized to preferentially isolate the monomeric form to keep the analysis consistent. The stoichiometry of binding (N), determined by ITC, is the number of DmsA leader peptide binding sites per DmsD protein molecule. One peptide (mean N value of >0.9) was shown to bind per DmsD molecule for WT and 11 of the 15 variant proteins (Table 3). Four DmsD variants (P124Q, W72S, F117A, and G78A) were shown to bind fewer than 1 peptide (mean N value of <0.9) per protein molecule, the values ranging from 0.81 (G78A) to 0.89 (P124Q). When the value of N is <1, it indicates that some portion of the protein population does not bind peptide. This could happen if some of the protein is present as dimers (with only one peptide binding site per 2 DmsD molecules) or if some portion of the protein population is folded in such a way as to be unable to bind peptide.

To understand if the multimeric composition of these DmsD variants was playing a role in the ITC-determined N value, size exclusion chromatography (SEC) was performed on select

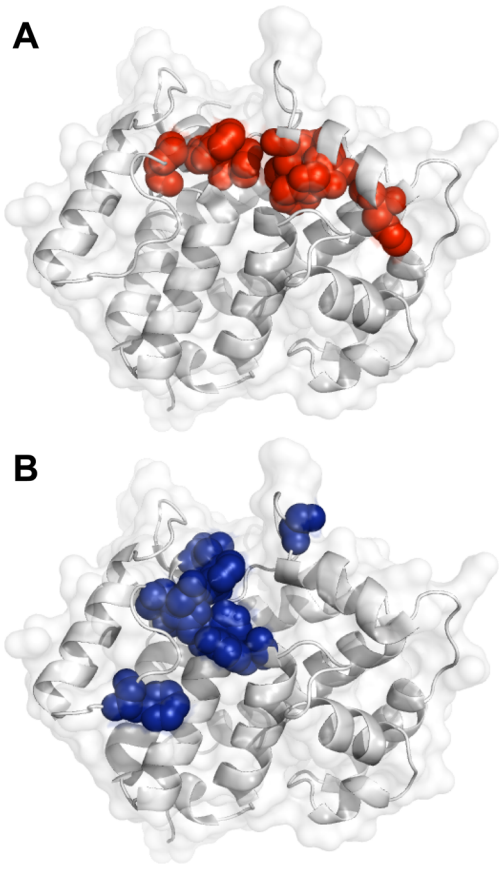

Figure 4. Increased flexibility in DmsD prior to binding DmsAL causes reduced affinity of DmsAL. Comparison of the entropy of binding for each DmsD variant residue relative to DmsD WT shown on a DmsD cartoon structure with variant residues represented as space-filling and colored according to a (A) higher (red) or (B) lower (blue) entropic cost of binding relative to that of WT. Mean values of entropy of binding of W72S and D126A DmsD were equivalent to that of WT DmsD (see Table 2), for the purpose of illustration; residues were colored according to the ITC results of more than two replicates.

DmsD variants (Table 3). Wild-type and selected variant DmsD proteins were resolved on a calibrated SEC column, allowing determination of the apparent molecular weight, multimeric state, and distribution of the eluted DmsD protein population. Sample chromatograms of DmsD proteins are shown in Figure 5A. All DmsD proteins (WT and variants) contained predominantly monomeric protein, which eluted with approximately 13.7 mL. A much smaller peak eluting with 12.3 mL was also present for all DmsD protein preparations and corresponded to dimeric protein. SEC was also performed on DmsD samples following ITC titration with $DmsAL_{15-41}$ peptide (Figure 5B) to determine if binding of the peptide caused a shift in the multimeric state of the protein present in solution.

For each SEC chromatogram, the area under all eluted peaks was calculated and totaled to determine the proportion of monomeric protein present in solution (Table 3). The total area under all protein peaks was similar for all resolved DmsD proteins and did not vary by more than 15% of the total (data not shown). The width at half-height of the monomeric peak was also consistent for all proteins. WT DmsD was shown to be 97% monomeric, but the value ranged from 95 to 100% (Table 3). W87S, D126A, and H127Y DmsD resolved like WT and

DOI: 10.1021/bi500891d
Biochemistry XXXX, XXX, XXX−XXX

Table 3. Number of Peptide Binding Sites, Monomeric Content, and Band Distribution of DmsD Variant Proteins Determined by ITC, SEC, and nPAGE Analyses

DmsD	N^a	monomer (%)^b (with DmsAL)^c	upper band^d
WT	1.04 ± 0.03	97 (96)	−/+
L75A	1.05 ± 0.05	nd^e	+
W87Y	1.03 ± 0.07	nd^e	−
H68Y	1.01 ± 0.03	nd^e	−
Y22F	1.00 ± 0.03	nd^e	−
V90N	0.99 ± 0.04	nd^e	−
W87S	0.96 ± 0.09	98 (98)	+
D126A	0.96 ± 0.07	97 (96)	+
H127Y	0.92 ± 0.02	96 (93)	+
P86Q	0.93 ± 0.12	91 (89)	+
F76A	0.94 ± 0.03	90 (85)	+
E123A	0.90 ± 0.06	86 (88)	+
P124Q	0.89 ± 0.04	85 (87)	+
W72S	0.87 ± 0.08	80 (78)	+
F117A	0.82 ± 0.04	nd^e	+
G78A	0.81 ± 0.15	65 (55)	+

$^a N$ is the mean number of $DmsAL_{15-41}$ peptide binding sites per DmsD protein molecule determined from ITC results. ^{b}Monomeric composition of DmsD protein in solution determined from the area under SEC-eluted protein peaks. ^{c}Monomeric composition of DmsD protein determined in the presence of a $DmsAL_{15-41}$ molar ratio of 2. ^{d}Upper band absent (−) or present (+) on nPAGE. ^{e}Not determined.

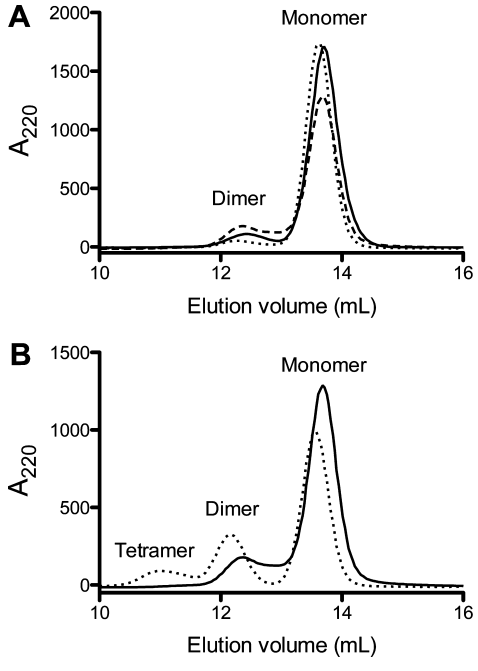

Figure 5. Size exclusion chromatography of DmsD proteins. DmsD proteins were resolved on a Superose 12 column and monitored at 220 nm (mAU). The total area under all eluted peaks was determined, and the monomer peak area (%) was analyzed for each DmsD variant and tabulated. (A) Sample chromatograms for WT DmsD (—), G78A (---), and W87S (···). (B) Sample chromatogram for DmsD G78A alone (—) and after addition of $DmsAL_{15-41}$ peptide (···).

were composed almost entirely of monomeric protein (Table 3). A slightly higher dimeric content (~10%) was found for P86Q and F76A DmsD. E123A, P124Q, W72S, and G78A DmsD proteins showed more than 15% dimeric protein. In the presence of DmsAL peptide, DmsD proteins showed approximately the same monomeric composition with variances between 1 and 5% (Table 3), and the position of the monomer peak shifted to a slightly earlier elution. The G78A DmsD variant contained the smallest amount of monomeric protein (65%) in the absence of peptide, showed the largest shift in composition (10% less monomer in the presence of peptide), and was the only variant protein that formed tetramers in addition to dimers in the presence of peptide (Figure 5B).

Native polyacrylamide gel electrophoresis (nPAGE) separates proteins on the basis of size and charge, allowing the resolution of multimeric complexes as well as proteins with different exposed charges. Native PAGE was used previously to show that DmsD exists in different folded forms despite being predominantly monomeric.[36] WT DmsD and variant proteins were resolved via nPAGE in the absence and presence of a reducing agent (Figure 6A,B). It is important to remember that DmsD proteins were prepared, purified, and stored in the presence of a reducing agent (DTT), but ITC and SEC experiments were conducted in the absence of DTT to remove any baseline effects. As such, nPAGE was presented for both conditions. In the absence of DTT, DmsD proteins are visualized as two bands on nPAGE, while in the presence of DTT, only a single band is visible (see arrows in Figure 6A,B). The most intense band(s) present for all DmsD proteins migrated near the middle of the nPAGE gel and was assumed to be representative of monomeric protein as this was the predominant form shown on SEC. The two DmsD variant proteins in which a single negative charge was removed from the protein (E123A and D126A) migrated slightly higher on the gel. Some DmsD proteins also showed a second band with a much lower intensity; migrating higher on the gel, this band was assumed to be representative of dimeric protein (Figure 6A,B). To compare the nPAGE results for each DmsD variant, the presence or absence of the upper (dimer) band was tabulated (Table 3). WT DmsD and variant proteins were also resolved via nPAGE in the presence of peptide; however, no differences were visible (data not shown).

When the ITC stoichiometry results, SEC monomeric content, and nPAGE results are compared (Table 3), further correlations can be made. WT DmsD and W87Y, H68Y, Y22F, and V90N variant proteins were shown by ITC to bind one peptide per protein molecule and contained no upper band on native PAGE (Table 3). These results are consistent with these proteins being monomeric in solution with a single peptide binding site. DmsD variant proteins L75A, W87S, D126A, H127Y, P86Q, and F76A bound one DmsA leader peptide per protein molecule, were composed of more than 90% monomeric protein, and presented an upper band on nPAGE. These variant proteins have some propensity to form dimers but bind a single peptide per protomer. DmsD variant proteins E123A, P124Q, W72S, and F117A bound between 0.8 and 0.9 DmsA leader peptide per DmsD molecule, are composed of 80−85% monomeric protein, and show an upper band on nPAGE. These variant proteins show a stronger propensity to form dimers and have a reduced binding stoichiometry. G78A DmsD is a mixed population of monomeric and dimeric protein, binds 0.8 DmsA leader peptide per molecule of DmsD, and shows two upper bands on nPAGE. G78A DmsD has the strongest propensity to dimerize, which in turn affects the number of DmsAL peptides that are able to bind, and tetramers form upon binding peptide.

DOI: 10.1021/bi500891d
Biochemistry XXXX, XXX, XXX−XXX

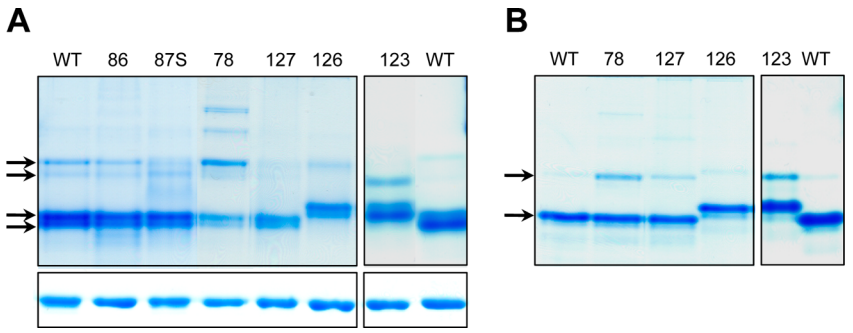

Figure 6. Native PAGE and SDS−PAGE resolution of DmsD proteins. WT DmsD and variant proteins (as indicated above each lane) were resolved via 12% nPAGE (top) or SDS−PAGE (bottom) and stained with Coomassie blue. Native PAGE was performed in the absence (A) or presence (B) of 100 mM DTT. Arrows indicate upper (dimer) and lower (monomer) protein band(s). The presence or absence of upper bands was determined and tabulated. E123A and D126A DmsD proteins migrate above WT and other DmsD variants because of the removal of one negative charge.

DISCUSSION

In this work, we have characterized the affinity, free energy, and contributions from enthalpy and entropy of 15 single-substitution DmsD variant proteins for a portion of the DmsAL peptide ($DmsAL_{15-41}$) substrate. The residues chosen for characterization are conserved within the DmsD family of proteins and localize to an indentation on or near the surface of the protein (Figure 1). The interaction between DmsD and this shortened portion of the DmsAL peptide ($DmsAL_{15-41}$) at pH 8.0 is driven by favorable enthalpy (−11.7 kcal/mol) but comes with an entropic cost (+3.7 kcal/mol). Many DmsD variant proteins bound to $DmsAL_{15-41}$ with a free energy similar to that of WT, but with large shifts in contributions from enthalpy and entropy. Substitution with hydrophobic residues Leu75, Trp87, or prolines Pro86 and Pro124 caused a 2-fold reduction in affinity between DmsD and $DmsAL_{15-41}$ because of the increased entropic cost of binding. The E123A DmsD variant showed the largest entropic shift and bound to the $DmsAL_{15-41}$ peptide with a favorable entropy (−1.8 kcal/mol), despite a binding affinity equivalent to that of WT DmsD. The reduced enthalpy and favorable entropy of binding support an interaction between this residue (Glu123) and the first arginine (R16) of the DmsAL peptide as suggested previously.[28]

The interaction between DmsD and the complete DmsAL peptide sequence fused to the N-terminus of either streptavidin binding peptide or glutathione *S*-transferase shows tight submicromolar binding. $DmsAL_{1-42}$::SBP bound to DmsD with a K_d of 0.06 μM at pH 7.4,[8] while the interaction between DmsD and a $DmsAL_{1-43}$::GST fusion was determined to be 3-fold weaker (K_d = 0.2 μM) at pH 8.0.[38] These results show how an almost identical DmsAL peptide ($DmsAL_{1-42}$ or $DmsAL_{1-43}$) fused to different partner proteins and assayed at different pH influences the interaction with DmsD. When smaller portions of the complete DmsAL peptide sequence were assayed for binding to DmsD, the tightest K_d (1.7 μM) was observed for the peptide used here ($DmsAL_{15-41}$).[24] When Ser15 and the first arginine (Arg16) were removed from the peptide, the level of binding to DmsD was reduced (K_d = 2.1 μM). The hydrophobic region ($DmsAL_{21-41}$), devoid of the entire twin-arginine motif, was shown to bind with an even weaker K_d of 3.9 μM. Those DmsD variants with the weakest binding to the $DmsAL_{15-41}$ peptide identified here bound with a similar affinity to the shortened DmsAL peptides and show support for disrupting the interaction with the twin-arginine motif specifically. To further test this possibility, ITC was performed with the E123A DmsD variant and the shortened DmsAL peptide ($DmsAL_{17-41}$). This DmsD variant bound this peptide with thermodynamic parameters almost identical to those of WT DmsD (ΔG = −7.7 kcal/mol, and K_d = 2.7 μM), including enthalpy (ΔH = −7.9 kcal/mol) and entropy ($-T\Delta S$ = +0.2 kcal/mol).[24] These results show support for residues of the DmsAL twin-arginine motif binding to the pocket of DmsD residues characterized here. The shift in entropy for DmsD E123A binding when Arg16 of the DmsAL peptide is present or absent further supports an interaction between Glu123 of DmsD and Arg16 of the DmsAL peptide as was also predicted from docking/simulation results.[28]

In our previous work that identified the RR leader binding site of DmsD, immunoblots were used to assay binding between DmsD variant proteins and the $DmsAL_{1-42}$::GST construct.[27] Seven DmsD variants (Y22F, H68Y, L75A, F76A, P86Q, E123A, and P124Q) showed similar results with both ITC and immunoblot. Four DmsD variants (W72S, W87Y, D126A, and H127Y) showed a different result with ITC from the immunoblot. W72S, D126A, and H127Y DmsD showed binding similar to WT binding with ITC but an approximately 5-fold reduction in the level of binding relative to that of WT DmsD with the immunoblot.[27] W87Y DmsD showed a slightly reduced level of binding by ITC but a 1.5-fold enhanced levelof binding with the immunoblot assay. One possibility is that the region of the DmsAL peptide not present in this ITC study (i.e., the 14 N-terminal amino acids) has more impact on binding these DmsD variants as was seen in the immunoblot assay that used the complete DmsAL sequence. Additionally, the original immunoblot assay used an overnight room-temperature incubation step, which the authors now believe magnified the impact of some of the DmsD variant proteins' stability. ITC experiments utilized protein that was maintained at 4 °C until immediately before the titrations were conducted. When the immunoblot assay was repeated without the overnight incubation, W72S, D126A, and H127Y DmsD proteins showed a higher level of binding; however, the levels were still reduced 2-fold relative to those of WT DmsD, and W87Y DmsD bound to a level almost identical to that of WT DmsD (data not shown).

Size exclusion chromatography and nPAGE results showed most DmsD variant proteins were composed of 85−95% monomeric protein, with the remainder of the population being dimeric. The G78A DmsD variant protein population was composed of the greatest amount of dimer (35%) and consequently the smallest amount of monomer (65%). In the presence of $DmsAL_{15-41}$ peptide, the G78A DmsD protein

DOI: 10.1021/bi500891d
Biochemistry XXXX, XXX, XXX−XXX

population shifted, even less protein was monomeric (55%), and tetramers were formed. Gly78 is found near Trp80, which forms a contact point in all three *E. coli* DmsD crystal structures, dimeric (PDB entry 3EFP),[28] tetrameric (PDB entry 3CWO),[32] and octameric (PDB entry 3U41). Additionally, the G78A DmsD variant showed the second tightest binding affinity (K_d = 1.2 μM) of all variant proteins studied here. DmsD and the homologous TorD protein have been shown to exist in different folded forms, which can be separated and visualized via nPAGE.[35,36] Each of the folded forms of DmsD was shown to bind to the DmsAL substrate,[38] and the *Shewanella massilia* TorD homologue, which crystallized as a domain-swapped dimer, showed binding to the TorA leader more efficient than that of the isolated monomer.[29,35]

The binding affinity of a related REMP protein, *E. coli* TorD, was studied in a similar but less robust manner.[26] TorD was shown to bind to its cognate TorA RR leader peptide with an affinity (K_d = 1.8 μM) similar to that of DmsD for the $DmsAL_{15-41}$ peptide used here (K_d = 1.7 μM). However, D124A and H125A TorD variants both had reduced binding affinity for the same TorAL peptide ($K_d \sim 5.0$ μM),[26] unlike what was found here for sequence equivalent residues in DmsD (D126A and H127Y), which had binding almost equivalent to that of WT DmsD (K_d = 1.6 μM). It is likely that the lower pH of the TorD experiments was the cause of the differences in affinity and possibly the presence of alternatively folded protein forms as seen in the nPAGE experiments. Alternatively, these residues found at the hinge point of the domain-swapped dimer might play different roles for DmsD and TorD. Additional support for the relevance of different folded forms within the family of REMPs was shown for the TorD homologue as only the domain-swapped dimer form of TorD was shown to have GTPase activity.[47]

In a study of the interaction between the homologous REMP, NarJ, and its substrate, the NarG peptide, ITC stoichiometry results were interpreted differently.[45] At lower pH (pH 7.0), when the stoichiometry values showed fewer than one binding site, it was concluded to be due to two forms of the NarJ protein, each with a different protonated state and each with different affinities for NarG.[45,46] At the higher pH of 8.0, NarJ bound to NarG with a reduced affinity but as a single population (presumably all the same protonated state) with a stoichiometry of 1:1. A similar interpretation must be considered for DmsD, as a subtle change in the protonation or the presence of an inter- or intramolecular salt bridge would influence the migration and charge/mass ratio on a nPAGE gel. The ITC experiments described in this study were conducted at pH 8.0 as DmsD WT and variants were prone to precipitation within the ITC experimental time frame when the pH was lowered to 7.0 (data not shown). To investigate if lowering the pH would cause a change in the thermodynamics, ITC experiments were attempted with WT DmsD and select variants at pH 7.5. WT DmsD showed slightly enhanced binding at pH 7.5 (K_d = 1.5 μM);e the levels of binding of D126A and H127Y were reduced ($K_d \sim 2-4$ μM), and the stoichiometry remained 1:1.

Without a structure of the DmsD−DmsAL complex, it is not possible to specify exactly where changes in entropy are occurring because the total entropy of binding consists of multiple components that may shift during the course of the formation of the complex.[48] The majority of favorable entropy is believed to be due to the release of water from the surface of a binding site; however, unfavorable entropy may be generated by the peptide as it changes from unstructured and flexible to a partially helical and bound state, as was suggested in our previous work.[24] The conformational entropy or the entropy gained or lost within the protein itself (due to a decreased or increased degree of freedom) is thought to be small as it is assumed that the protein structure becomes more rigid upon binding its substrate. In fact, upon binding, most peptides do not induce conformational changes in their partner protein, minimizing this entropic cost.[49] In the studies presented here, involving a portion of the DmsA twin-arginine leader peptide, it would follow that DmsD does not undergo much conformational change upon binding the peptide. Our previous study shows support for a minimal conformational change in DmsD upon binding at pH 8.0, as the melting temperature of DmsD increased by <1 °C when it was in complex with the same peptide used here over that of the melting temperature of the DmsD protein alone.[24]

For those DmsD variant proteins that showed binding weaker than that of WT DmsD, the higher entropic cost of binding caused the greatest free energy loss. In these cases, more order is found within the complex and surrounding solvent than in the separate DmsD and DmsAL peptide in solution.[24] The increased entropic cost is localized to helix 5 residues (His68, Trp72, Leu75, and Phe76) and two Prolines (Pro86 and Pro124) and when Trp87 is changed to a serine. The increased entropic cost of binding for these residues (Figure 4A) suggests that the substitutions cause this region of the binding site to become more flexible, relative to the WT DmsD, prior to binding. In contrast, substitutions with residues other than proline, found on loops, reduced the entropic cost of binding, suggesting a more rigid conformation in DmsD, caused by the substitution. From these results, we can postulate that maintaining the structure of helix 5 in DmsD plays a role in the stabilization of binding due to entropy, potentially through hydrophobic interactions with neighboring DmsD residues positioning helix 5. These results together suggest that the region of DmsD binding the twin-arginine motif is more rigid and defined because substitutions that increased flexibility also reduced the affinity and substitutions that reduced flexibility enhanced the affinity. One particular loop (following helix 5) contains four prolines (two of which are highly conserved among the DmsD family of proteins) and also appears to be important. The reduced degree of conformational freedom provided by the four prolines within this loop may be important for binding between DmsD and DmsAL peptide. In fact, when Pro86 was changed to a glutamine, the level of binding was reduced 2-fold. A variant protein of the other conserved proline within this loop (Pro85) was also made; however, this protein routinely precipitated during ITC titrations, so thermodynamics were unable to be determined. The initial heat values for a P85Q titration were very similar to those of P86Q, and an immunoblot assay of the P85Q DmsD variant showed DmsAL peptide binding levels almost identical to that of the P86Q variant (data not shown).

A recent NMR study investigated the chemical shift changes of residues in DmsD by comparison of DmsD alone and DmsD in complex with a $DmsAL_{1-44}$ peptide fused to DmsD at an undefined ratio and pH 6.5.[44] The data are promising; however, a substantial number of residues could not be assigned, including all 14 prolines and most of the residues within the putative binding site, and the greatest chemical shifts were in a nearby region (Table 1 and Figure S2 of the Supporting Information). Additionally, 63 residues clustering near helix 5

DOI: 10.1021/bi500891d
Biochemistry XXXX, XXX, XXX−XXX

showed conformational heterogeneity.[44] Comparison of the DmsD structure with the mapped chemical shifts upon binding $DmsAL_{1-44}$, and the entropic shifts determined here, shown both without and with the docked DmsAL peptide, allows for some speculation (Figure S2 of the Supporting Information). The largest chemical shifts occur along a groove in the protein below the putative twin-arginine motif binding site (Figure S2A of the Supporting Information). One residue in particular with the largest chemical shift (Phe117) is included within this groove. The authors believe that this hydrophobic cleft of DmsD binds the hydrophobic region of the DmsAL peptide, which is also less conserved than the twin-arginine motif. F117A DmsD was the tightest binding variant characterized here, and all free energy gain was due to favorable entropy, supporting this theory.

The DmsD residues binding the twin-arginine motif are highly conserved across the DmsD/TorD protein family. Unresolved density found within DmsD crystals[32] as well as a docked peptide structure provides further support for the pocket of DmsD characterized here binding to the conserved twin-arginine motif.[28,50] The ITC results suggest that any substitutions, which increase the flexibility within this area, reduce binding affinity. It is likely that there is in fact very little conformational change in this region of DmsD upon binding the DmsAL peptide and that any conformational changes in DmsD that do occur are located near the position where the hydrophobic region of DmsAL binds.[44,50,51]

It is possible that the DmsD variant proteins may stabilize different folding forms and/or populations, and as a result, we observe different affinities. Our previous hypothesis that DmsD, a Tat system specific chaperone, interacts with other general chaperones as well as proteins involved in molybdopterin cofactor biosynthesis[52] would suggest that DmsD and other REMPs interact with multiple proteins while escorting their enzyme substrate through folding and then docking to the Tat translocase. The different folding forms with different affinity states may be key to this process, and the subtle localized pH changes within the cell may also play a role.

CONCLUSIONS

The highly conserved "hot pocket" residues of the DmsD chaperone characterized here likely form the binding site for the twin-arginine motif (SRRGLVK) of the DmsAL peptide, a finding also supported by previous studies.[28,50] The results show evidence of an interaction between the first arginine (Arg16) of the DmsAL twin-arginine motif and Glu123 of DmsD. Overall, only one DmsD variant increased the free energy of binding by more than 0.5 kcal/mol and, as such, qualified as a key "hot spot" identifier.[49,53,54] The hydrophobic region of the DmsAL peptide likely binds across a larger, less conserved, and as yet ill-defined surface on DmsD.

ASSOCIATED CONTENT

Supporting Information

Sample ITC thermograms of DmsD variants binding to $DmsAL_{15-41}$ and structures of DmsD with mapped chemical shifts and entropic changes of binding (Figures S1 and S2). This material is available free of charge via the Internet at http://pubs.acs.org.

AUTHOR INFORMATION

Corresponding Author

*E-mail: turnerr@ucalgary.ca. Telephone: (403) 220-4308.

Funding

This work was supported by an operating grant to R.J.T. from the Canadian Institutes of Health Research and a Canada Graduate Scholarship to T.M.L.W. from the Natural Sciences and Engineering Research Council of Canada.

Notes

The authors declare no competing financial interest.

ACKNOWLEDGMENTS

We thank Siyuan Wang and Stephana Cherak for technical assistance.

ABBREVIATIONS

DmsAL, DmsA leader peptide; ΔG, change in Gibbs free energy; ΔH, change in enthalpy; ΔS, change in entropy; DMSO, dimethyl sulfoxide; ITC, isothermal titration calorimetry; K_d, dissociation constant; MoPt, molybdopterin; nPAGE, native polyacrylamide gel electrophoresis; REMP, redox enzyme maturation protein; RR, twin-arginine; SDS–PAGE, sodium dodecyl sulfate–polyacrylamide gel electrophoresis; SEC, size exclusion chromatography; Tat, twin-arginine translocase; WT, wild type.

REFERENCES

(1) Weiner, J. H., Bilous, P. T., Shaw, G. M., Lubitz, S. P., Frost, L., Thomas, G. H., Cole, J. A., and Turner, R. J. (1998) A novel and ubiquitous system for membrane targeting and secretion of cofactor-containing proteins. *Cell 93*, 93–101.

(2) Sargent, F., Bogsch, E., Stanley, N., Wexler, M., Robinson, C., Berks, B., and Palmer, T. (1998) Overlapping functions of components of a bacterial Sec-independent protein export pathway. *EMBO J. 17*, 3640–3650.

(3) Berks, B. C., Palmer, T., and Sargent, F. (2003) The Tat protein translocation pathway and its role in microbial physiology. In *Advances in Microbial Physiology*, Vol. *47*, pp 187–254, Academic Press Ltd., London.

(4) Lee, P. A., Tullman-Ercek, D., and Georgiou, G. (2006) The bacterial twin-arginine translocation pathway. *Annu. Rev. Microbiol. 60*, 373–395.

(5) Palmer, T., and Berks, B. C. (2012) The twin-arginine translocation (Tat) protein export pathway. *Nat. Rev. Microbiol. 10*, 483–496.

(6) Magalon, A., Fedor, J. G., Walburger, A., and Weiner, J. H. (2011) Molybdenum enzymes in bacteria and their maturation. *Coord. Chem. Rev. 255*, 1159–1178.

(7) Sargent, F. (2007) Constructing the wonders of the bacterial world: Biosynthesis of complex enzymes. *Microbiology 153*, 633–651.

(8) Chan, C. S., Chang, L., Rommens, K. L., and Turner, R. J. (2009) Differential interactions between Tat-specific redox enzyme peptides and their chaperones. *J. Bacteriol. 191*, 2091–2101.

(9) Chan, C. S., Chang, L., Winstone, T. M., and Turner, R. J. (2010) Comparing system-specific chaperone interactions with their Tat dependent redox enzyme substrates. *FEBS Lett. 584*, 4553–4558.

(10) Turner, R. J., Papish, A. L., and Sargent, F. (2004) Sequence analysis of bacterial redox enzyme maturation proteins (REMPs). *Can. J. Microbiol. 50*, 225–238.

(11) Oresnik, I. J., Ladner, C. L., and Turner, R. J. (2001) Identification of a twin-arginine leader-binding protein. *Mol. Microbiol. 40*, 323–331.

(12) Ray, N., Oates, J., Turner, R. J., and Robinson, C. (2003) DmsD is required for the biogenesis of DMSO reductase in *Escherichia coli* but not for the interaction of the DmsA signal peptide with the Tat apparatus. *FEBS Lett. 534*, 156–160.

(13) Pommier, J., Mejean, V., Giordano, G., and Iobbi-Nivol, C. (1998) TorD, a cytoplasmic chaperone that interacts with the

DOI: 10.1021/bi500891d
Biochemistry XXXX, XXX, XXX–XXX

unfolded trimethylamine N-oxide reductase enzyme (TorA) in *Escherichia coli*. *J. Biol. Chem. 273*, 16615−16620.
(14) Shaw, A. L., Leimkuhler, S., Klipp, W., Hanson, G. R., and McEwan, A. G. (1999) Mutational analysis of the dimethylsulfoxide respiratory (dor) operon of *Rhodobacter capsulatus*. *Microbiology 145* (Part 6), 1409−1420.
(15) Ilbert, M., Mejean, V., Giudici-Orticoni, M. T., Samama, J. P., and Iobbi-Nivol, C. (2003) Involvement of a mate chaperone (TorD) in the maturation pathway of molybdoenzyme TorA. *J. Biol. Chem. 278*, 28787−28792.
(16) Genest, O., Ilbert, M., Mejean, V., and Iobbi-Nivol, C. (2005) TorD, an essential chaperone for TorA molybdoenzyme maturation at high temperature. *J. Biol. Chem. 280*, 15644−15648.
(17) Genest, O., Seduk, F., Ilbert, M., Mejean, V., and Iobbi-Nivol, C. (2006) Signal peptide protection by specific chaperone. *Biochem. Biophys. Res. Commun. 339*, 991−995.
(18) Genest, O., Seduk, F., Theraulaz, L., Mejean, V., and Iobbi-Nivol, C. (2006) Chaperone protection of immature molybdoenzyme during molybdenum cofactor limitation. *FEMS Microbiol. Lett. 265*, 51−55.
(19) Dow, J. M., Gabel, F., Sargent, F., and Palmer, T. (2013) Characterization of a pre-export enzyme-chaperone complex on the twin-arginine transport pathway. *Biochem. J. 452*, 57−66.
(20) Blasco, F., Dos Santos, J. P., Magalon, A., Frixon, C., Guigliarelli, B., Santini, C. L., and Giordano, G. (1998) NarJ is a specific chaperone required for molybdenum cofactor assembly in nitrate reductase A of *Escherichia coli*. *Mol. Microbiol. 28*, 435−447.
(21) Liu, X., and DeMoss, J. A. (1997) Characterization of NarJ, a system-specific chaperone required for nitrate reductase biogenesis in *Escherichia coli*. *J. Biol. Chem. 272*, 24266−24271.
(22) Sodergren, E. J., Hsu, P. Y., and DeMoss, J. A. (1988) Roles of the narJ and narI gene products in the expression of nitrate reductase in *Escherichia coli*. *J. Biol. Chem. 263*, 16156−16162.
(23) Chan, C. S., Howell, J. M., Workentine, M. L., and Turner, R. J. (2006) Twin-arginine translocase may have a role in the chaperone function of NarJ from *Escherichia coli*. *Biochem. Biophys. Res. Commun. 343*, 244−251.
(24) Winstone, T. M., Tran, V. A., and Turner, R. J. (2013) The Hydrophobic Region of the DmsA Twin-Arginine Leader Peptide Determines Specificity with Chaperone DmsD. *Biochemistry 52*, 7532−7541.
(25) Shanmugham, A., Bakayan, A., Voller, P., Grosveld, J., Lill, H., and Bollen, Y. J. (2012) The hydrophobic core of twin-arginine signal sequences orchestrates specific binding to Tat-pathway related chaperones. *PLoS One 7*, e34159.
(26) Hatzixanthis, K., Clarke, T. A., Oubrie, A., Richardson, D. J., Turner, R. J., and Sargent, F. (2005) Signal peptide-chaperone interactions on the twin-arginine protein transport pathway. *Proc. Natl. Acad. Sci. U.S.A. 102*, 8460−8465.
(27) Chan, C. S., Winstone, T. M. L., Chang, L., Stevens, C. M., Workentine, M. L., Li, H., Wei, Y., Ondrechen, M. J., Paetzel, M., and Turner, R. J. (2008) Identification of residues in DmsD for twin-arginine leader peptide binding, defined through random and bioinformatics-directed mutagenesis. *Biochemistry 47*, 2749−2459.
(28) Stevens, C. M., Winstone, T. M., Turner, R. J., and Paetzel, M. (2009) Structural analysis of a monomeric form of the twin-arginine leader peptide binding chaperone *Escherichia coli* DmsD. *J. Mol. Biol. 389*, 124−133.
(29) Tranier, S., Iobbi-Nivol, C., Birck, C., Ilbert, M., Mortier-Barriere, I., Mejean, V., and Samama, J. P. (2003) A novel protein fold and extreme domain swapping in the dimeric TorD chaperone from *Shewanella massilia*. *Structure 11*, 165−174.
(30) Kirillova, O., Chruszcz, M., Shumilin, I. A., Skarina, T., Gorodichtchenskaia, E., Cymborowski, M., Savchenko, A., Edwards, A., and Minor, W. (2007) An extremely SAD case: Structure of a putative redox-enzyme maturation protein from *Archaeoglobus fulgidus* at 3.4 Å resolution. *Acta Crystallogr. D63*, 348−354.
(31) Qiu, Y., Zhang, R., Binkowski, T. A., Tereshko, V., Joachimiak, A., and Kossiakoff, A. (2008) The 1.38 Å crystal structure of DmsD protein from *Salmonella typhimurium*, a proofreading chaperone on the Tat pathway. *Proteins 71*, 525−533.
(32) Ramasamy, S. K., and Clemons, W. M., Jr. (2009) Structure of the twin-arginine signal-binding protein DmsD from *Escherichia coli*. *Acta Crystallogr. F65*, 746−750.
(33) Jack, R. L., Buchanan, G., Dubini, A., Hatzixanthis, K., Palmer, T., and Sargent, F. (2004) Coordinating assembly and export of complex bacterial proteins. *EMBO J. 23*, 3962−3972.
(34) Ilbert, M., Mejean, V., and Iobbi-Nivol, C. (2004) Functional and structural analysis of members of the TorD family, a large chaperone family dedicated to molybdoproteins. *Microbiology 150*, 935−943.
(35) Tranier, S., Mortier-Barriere, I., Ilbert, M., Birck, C., Iobbi-Nivol, C., Mejean, V., and Samama, J. P. (2002) Characterization and multiple molecular forms of TorD from *Shewanella massilia*, the putative chaperone of the molybdoenzyme TorA. *Protein Sci. 11*, 2148−2157.
(36) Sarfo, K. J., Winstone, T. L., Papish, A. L., Howell, J. M., Kadir, H., Vogel, H. J., and Turner, R. J. (2004) Folding forms of *Escherichia coli* DmsD, a twin-arginine leader binding protein. *Biochem. Biophys. Res. Commun. 315*, 397−403.
(37) Bordo, D., and Argos, P. (1991) Suggestions for "safe" residue substitutions in site-directed mutagenesis. *J. Mol. Biol. 217*, 721−729.
(38) Winstone, T. L., Workentine, M. L., Sarfo, K. J., Binding, A. J., Haslam, B. D., and Turner, R. J. (2006) Physical nature of signal peptide binding to DmsD. *Arch. Biochem. Biophys. 455*, 89−97.
(39) Hanahan, D. (1983) Studies on transformation of *Escherichia coli* with plasmids. *J. Mol. Biol. 166*, 557−580.
(40) Gasteiger, E., Hoogland, C., Gattiker, A., Duvaud, S., Wilkins, M. R., Appel, R. D., and Bairoch, A. (2005) Protein Identification and Analysis Tools on the ExPASy Server. In *The Proteomics Protocols Handbook* (Walker, J. M., Ed.) pp 571−607, Humana Press, Totowa, NJ.
(41) Gallagher, S. R. (2006) One-dimensional SDS gel electrophoresis of proteins. *Current Protocols in Molecular Biology*, Chapter 10, Unit 10, 12A, Wiley, New York.
(42) Laemmli, U. K. (1970) Cleavage of structural proteins during the assembly of the head of bacteriophage T4. *Nature 227*, 680−685.
(43) DeLano, W. L. (2002) *The PyMOL Molecular Graphics System*, version 1.0r1, DeLano Scientific, San Carlos, CA.
(44) Stevens, C. M., Okon, M., McIntosh, L. P., and Paetzel, M. (2013) ^{1}H, ^{13}C and ^{15}N resonance assignments and peptide binding site chemical shift perturbation mapping for the *Escherichia coli* redox enzyme chaperone DmsD. *Biomol. NMR Assignments 7*, 193−197.
(45) Zakian, S., Lafitte, D., Vergnes, A., Pimentel, C., Sebban-Kreuzer, C., Toci, R., Claude, J. B., Guerlesquin, F., and Magalon, A. (2010) Basis of recognition between the NarJ chaperone and the N-terminus of the NarG subunit from *Escherichia coli* nitrate reductase. *FEBS J. 277*, 1886−1895.
(46) Lorenzi, M., Sylvi, L., Gerbaud, G., Mileo, E., Halgand, F., Walburger, A., Vezin, H., Belle, V., Guigliarelli, B., and Magalon, A. (2012) Conformational selection underlies recognition of a molybdoenzyme by its dedicated chaperone. *PLoS One 7*, e49523.
(47) Guymer, D., Maillard, J., Agacan, M. F., Brearley, C. A., and Sargent, F. (2010) Intrinsic GTPase activity of a bacterial twin-arginine translocation proofreading chaperone induced by domain swapping. *FEBS J. 277*, 511−525.
(48) Reichmann, D., Rahat, O., Cohen, M., Neuvirth, H., and Schreiber, G. (2007) The molecular architecture of protein-protein binding sites. *Curr. Opin. Struct. Biol. 17*, 67−76.
(49) London, N., Movshovitz-Attias, D., and Schueler-Furman, O. (2010) The structural basis of peptide-protein binding strategies. *Structure 18*, 188−199.
(50) Stevens, C. M. (2012) Structural and Computational Analysis of the *Escherichia coli* Chaperone Protein DmsD. Department of Molecular Biology & Biochemistry, Simon Fraser University, Burnaby, BC.

DOI: 10.1021/bi500891d
Biochemistry XXXX, XXX, XXX−XXX

(51) Stevens, C. M., and Paetzel, M. (2012) Purification of a Tat leader peptide by co-expression with its chaperone. *Protein Expression Purif. 84*, 167−172.
(52) Li, H., Chang, L., Howell, J. M., and Turner, R. J. (2010) DmsD, a Tat system specific chaperone, interacts with other general chaperones and proteins involved in the molybdenum cofactor biosynthesis. *Biochim. Biophys. Acta 1804*, 1301−1309.
(53) Thorn, K. S., and Bogan, A. A. (2001) ASEdb: A database of alanine mutations and their effects on the free energy of binding in protein interactions. *Bioinformatics 17*, 284−285.
(54) Bogan, A. A., and Thorn, K. S. (1998) Anatomy of hot spots in protein interfaces. *J. Mol. Biol. 280*, 1−9.

DOI: 10.1021/bi500891d
Biochemistry XXXX, XXX, XXX−XXX